Experimental Neurology xxx (2010) xxx–xxx

Contents lists available at ScienceDirect

Experimental Neurology

journal homepage: www.elsevier.com/locate/yexnr

Mitochondrial-dependent apoptosis in Huntington's disease human cybrids

Ildete L. Ferreira [a], Maria V. Nascimento [a], Márcio Ribeiro [a], Sandra Almeida [a], Sandra M. Cardoso [a], Manuela Grazina [a,b], João Pratas [a], Maria João Santos [a], Cristina Januário [c], Catarina R. Oliveira [a,b], A. Cristina Rego [a,b,*]

[a] Center for Neuroscience and Cell Biology, Faculty of Medicine, University of Coimbra, Portugal
[b] Institute of Biochemistry, Faculty of Medicine, University of Coimbra, Portugal
[c] Neurology Unit, Coimbra University Hospital, Coimbra, Portugal

ARTICLE INFO

Article history:
Received 10 September 2009
Revised 26 November 2009
Accepted 5 January 2010
Available online xxxx

Keywords:
Apoptosis
Human cybrids
Huntington's disease
Mitochondria
3-Nitropropionic acid

ABSTRACT

We investigated the involvement of mitochondrial-dependent apoptosis in Huntington's disease (HD) vs. control (CTR) cybrids, obtained from the fusion of human platelets with mitochondrial DNA-depleted NT2 cells, and further exposed to 3-nitropropionic acid (3-NP) or staurosporine (STS). Untreated HD cybrids did not exhibit significant modifications in the activity of mitochondrial respiratory chain complexes I–IV or in mtDNA sequence variations suggestive of a primary role in mitochondrial susceptibility in the subpopulation of HD carriers studied. However, a slight decrease in mitochondrial membrane potential and increased formation of intracellular hydroperoxides was observed in HD cybrids under basal conditions. Furthermore, apoptotic nuclei morphology and a moderate increase in caspase-3 activation, as well as increased levels of superoxide ions and hydroperoxides were observed in HD cybrids upon 3-NP or STS treatment. 3-NP-evoked apoptosis in HD cybrids involved cytochrome c and AIF release from mitochondria, which was associated with mitochondrial Bax translocation. CTR cybrids subjected to 3-NP showed increased mitochondrial Bax and Bim levels and the release of AIF, but not cytochrome c, suggesting a different mode of cell death, linked to the loss of membrane integrity. Additionally, increased mitochondrial Bim and Bak levels, and a slight release of cytochrome c in untreated HD cybrids may help to explain their moderate susceptibility to mitochondrial-dependent apoptosis.

Introduction

Huntington's disease (HD) is an autosomal dominant disorder characterized by uncontrolled body movements known as chorea, changes in personality and a loss of cognitive ability eventually leading to dementia. HD is caused by an expansion of the trinucleotide CAG repeat in the huntingtin gene, producing a protein with increased number of polyglutamines at the N-terminal (mutant huntingtin). Neuropathological changes are caused by the death of GABAergic projection medium-spiny neurons of the neostriatum (caudate and putamen) and neurons in the cerebral cortex, the two most severely affected brain structures in HD (e.g., Gil and Rego, 2008). However, the mechanisms by which mutant huntingtin causes selective degeneration of striatal and cortical neurons in HD are largely unknown.

Neuronal abnormalities involving aberrant protein–protein interactions caused by mutant huntingtin may lead to deregulation in gene expression in human HD striatum (Kuhn et al., 2007). Furthermore, excitotoxicity linked to decreased Ca^{2+} homeostasis, mitochondrial dysfunction, impairment in energy metabolism (Schapira, 1998; Beal, 2005; Sas et al., 2007; Sorolla et al., 2008; Yang et al., 2008), caspase activation and apoptosis (Brouillet et al., 1998; Beal, 2005; Milakovic and Johnson, 2005; Rego and de Almeida, 2005; Fan and Raymond, 2007) have been reported in HD-affected individuals. In addition, oxidative stress and damage to specific macromolecules also participate in HD progression (Sorolla et al., 2008).

Analysis of post-mortem striatal tissue from HD patients revealed a decrease in the activity of the respiratory chain complexes II/III and IV (Schapira 1998; Tabrizi et al., 1999). Mutant huntingtin may cause mitochondrial dysfunction by either perturbing transcription of nuclear-encoded mitochondrial proteins or by directly interacting with the organelle, thus evoking defects in mitochondrial dynamics, organelle trafficking and fission and fusion, which, in turn, may result in bioenergetic failure in HD (Bossy-Wetzel et al., 2008). Indeed, mild or gradual energy disturbances may lead to the release of pro-apoptotic factors from the mitochondria, such as cytochrome c, leading to apoptotic cell death. However, if the energy supply of the cell drops dramatically, cells die by necrosis (Vanlangenakker et al., 2008).

* Corresponding author. Center for Neuroscience and Cell Biology, and Institute of Biochemistry, Faculty of Medicine, Ruas Larga, University of Coimbra, 3004-504 Coimbra, Portugal. Fax: +351 239 822776.
E-mail addresses: a.cristina.rego@gmail.com, acrego@cnc.cj.uc.pt (A.C. Rego).

0014-4886/$ – see front matter © 2010 Published by Elsevier Inc.
doi:10.1016/j.expneurol.2010.01.002

Mutant huntingtin is widely expressed in the HD brain (Aronin et al., 1995; Trottier et al., 1995), but also in peripheral tissues. Thus, abnormalities outside the brain can also be expected. Accordingly, mutant huntingtin was reported to be associated with mitochondrial complex II/III dysfunction, mitochondrial depolarization, cytochrome c release and increased caspases activity in skeletal muscle (Ciammola et al., 2006; Turner et al., 2007), and decreased catalase activity in skin fibroblast cultures from HD patients (del Hoyo et al., 2006). Lymphoblasts derived from HD patients also show increased stress-induced apoptotic cell death associated with caspase-3 activation, abnormal calcium homeostasis and mitochondrial dysfunction (Sawa et al., 1999; Panov et al., 2002; Bezprozvanny and Hayden, 2004). Recently, we demonstrated that HD human peripheral blood cells, particularly B lymphocytes, are endowed with increased expression of Bax and decreased mitochondrial membrane potential (Almeida et al., 2008), further suggesting that an adverse effect of mutant huntingtin is not limited to neurons.

It is widely accepted that mitochondrial DNA (mtDNA) abnormalities play an important role in neurodegenerative diseases (Grazina et al., 2006; Onyango et al., 2006), even if they are not a primary triggering factor (Mancuso et al., 2008). mtDNA mutations may modify the age of onset, as a result of an impairment of mitochondrial respiratory chain and/or translational mechanisms thus contributing to the neurodegenerative process (Grazina et al., 2006). Even though the studies concerning HD and mtDNA mutations are rare and heterogeneous, mtDNA mutations have been suggested to occur in HD pathophysiology (Kasraie et al., 2008; Yang et al., 2008). It was recently demonstrated that mitochondrial DNA damage is an early biomarker for HD-associated neurodegeneration supporting the hypothesis that mtDNA lesions may contribute to the pathogenesis observed in HD (Acevedo-Torres et al., 2009). Indeed, recent data showed that HD patients' lymphocytes have higher frequencies of mtDNA deletions and oxidative stress, suggesting that CAG repeats instability and mutant huntingtin are a causative factor in mtDNA damage (Banoei et al., 2007). Nevertheless, previous studies in HD cybrids (a valuable cellular tool to isolate mitochondrial-encoded human defects) showed no changes in mitochondrial respiratory chain activity or oxidative stress (Swerdlow et al., 1999), evidencing no major changes in mitochondrial function, even if considering the occurrence of point mtDNA mutations. Notwithstanding, mutant huntingtin was previously shown to interact with neuronal mitochondria of YAC72 transgenic mice suggesting that mitochondrial calcium abnormalities associated with HD pathogenesis may be due to a direct effect of mutant huntingtin on the organelle (Panov et al., 2002). Moreover, mutant huntingtin fragments can directly induce the opening of the mitochondrial permeability transition pore in isolated mouse liver mitochondria, with the consequent release of cytochrome c (Choo et al., 2004), favoring the hypothesis that mutant huntingtin interacting with mitochondria may well lead to mitochondrial modifications independently of damage on mtDNA.

Thus, in the present study, we studied mitochondrial-dependent apoptotic events and oxidative stress in human cybrid lines, obtained from the fusion of HD or control platelets with NT2 ρ^0 cells, depleted of mitochondrial DNA. We report increased susceptibility of a subpopulation of HD cybrids, an *ex vivo* mitochondrial HD human model, to undergo mitochondrial-dependent apoptosis when subjected to complex II inhibition with 3-nitropropionic acid (3-NP) or to apoptosis with the classic inducer staurosporine (STS).

Materials and methods

Materials

Optimem was purchased from GIBCO (Paisley, UK). Protease inhibitor cocktail (chymostatin, pepstatin, A, leupeptin and antipain), 3-nitropropionic acid, penicillin/streptomycin, oligomycin, carbonyl-cyanide-*p*-(trifluoromethoxyphenyl)hydrazone (FCCP), dichlorphenolindophenol (DCPIP), thenoyltrifluoroacetone (TTFA), 5,59-dithiobis (2-nitrobenzoic acid) (DTNB) and anti-α-tubulin were from Sigma Chemical Co. (St Louis, MO, USA). *N*-acetyl-Asp-Glu-Val-Asp-*p*-nitroanilide (Ac-DEVD-pNA) was obtained from Calbiochem (Darmstadt, Germany). Anti-cytochrome c was from BD Pharmingen (San Diego, CA, USA); anti-Bax from Cell Signaling (Beverly, MA, USA); anti-Bcl-2 and anti-AIF from Santa Cruz Biotechnology (Santa Cruz, CA, USA); anti-Bim from Stressgen (Assay Designs, Inc., Michigan, USA); and anti-Bak from Abcam Inc. (Cambridge, USA). Secondary antibodies conjugated to alkaline phosphatase (anti-mouse and anti-rabbit) were purchased from Amersham Biosciences (Buckinghamshire, UK). The fluorescence probes tetramethylrhodamine methyl ester (TMRM+), dihydroethidium (DHE), 2′,7′-dichlorodihydrofluorescein diacetate ($DCFH_2$-DA), Hoechst 33342 and anti-cytochrome c oxidase I (COX I) were obtained from Molecular Probes (Invitrogen, USA). All other reagents were of analytical grade.

Participants

Five to six genetically and clinically confirmed HD patients from pre-identified Portuguese families and three age-matched healthy controls, without any neurological disease, were studied. The number of CAG repeats present in HD gene for all the patients were between 42 and 44, which gives rise to the most common adult-onset form of the disease. The patients were characterized according to the Unified Huntington's Disease Rating Scale (UHDRS) (Huntington Study Group, 1996) and neurological evaluation was performed by an experienced neurologist. The study was performed in accordance with the Ethical Committee of Coimbra University Hospital, and all the subjects gave informed consent.

Cybrid production, culture and incubation with 3-NP and STS

Cybrids (cytoplasmic hybrid systems) were produced after fusion of mitochondrial DNA-depleted human teratocarcinoma cells (ρ° NT2 cells), obtained from Dr. R. H. Swerdlow (University of Virginia, Charlottesville, VA, USA), with human platelets. Production and selection of the cybrids were performed as described previously (Cardoso et al., 2004). Cybrids were cultured in Optimem medium supplemented with 10% of fetal calf serum, penicillin (100 U/ml), streptomycin (100 μg/ml) and maintained at 37 °C in humidified incubator containing 95% air and 5% CO_2. Since mitochondria divide mainly in response to the energy needs of the cell, i.e., independently of the cell cycle (Sas et al., 2007) and to account for the auto-selection of the remaining functional mitochondria, experiments were performed with cybrids less than 2 months in culture, as previously described (e.g., Cardoso et al., 2004). Cybrids were plated on glass coverslips, multiwell chambers or flasks at a density of 0.06×10^6 cells/cm^2 one day before the experiments in order to allow the desired confluence. Cells were then incubated in culture medium in the absence or presence of 3-NP (0.1, 1 or 10 mM) for 24 h or STS (0.1, 1 or 10 nM) for 15 h, as described in figure legends.

Assay of enzymatic activities of mitochondrial electron transport chain

Cybrids were extracted in a sucrose buffer (250 mM sucrose; 20 mM HEPES-KOH, pH 7.5; 100 mM KCl; 1.5 mM $MgCl_2$; 1 mM EDTA and 1 mM EGTA), and centrifuged at 2300 rpm for 12 min at 4 °C. The supernatant was analyzed for mitochondrial complex activities on a UV/VIS spectrophotometer (model 2401; Shimadzu Scientific Instruments, Columbia, MD).

NADH–ubiquinone oxidoreductase assay

Complex I activity was determined at 340 nm by following the decrease in NADH absorbance that occurs when ubiquinone is

Please cite this article as: Ferreira, I.L., et al., Mitochondrial-dependent apoptosis in Huntington's disease human cybrids, Exp. Neurol. (2010), doi:10.1016/j.expneurol.2010.01.002

reduced to ubiquinol. The reaction was started by adding the sample to the reaction mixture (in mM: 20 K_2HPO_4, pH 7.2, 10 $MgCl_2$, 0.15 NADH, 2.5 mg/ml BSA fatty-acid free, 1 KCN) containing 50 μM decylubiquinone, at 30 °C. After 8 min, rotenone (10 μM) was added and the reaction was registered for further 8 min. Complex I activity was expressed in nanomoles per minute per milligram of protein and correspond to the rotenone sensitive rate. The enzyme activity was corrected for citrate synthase activity.

Succinate–ubiquinone oxidoreductase assay

Complex II activity was monitored at 600 nm by following the reduction of 6,6-dichlorophenolindophenol (DCPIP) by the ubiquinol formed in the reaction. The assay was started by adding the sample to the reaction mixture (in mM: 50 K_2HPO_4, pH 7.4, 20 succinate, 0.1 EDTA, 1 KCN, 0.01 rotenone) containing 50 μM decylubiquinone, at 30 °C. After 8 min, 1 mM 2-thenoyltrifluoroacetone (TTFA) was added and the reaction registered for further 8 min. Complex II activity was expressed in nanomoles per minute per milligram of protein and correspond to the TTFA sensitive rate. The enzyme activity was corrected for citrate synthase activity.

Ubiquinol–cytochrome c reductase assay

Complex III activity was monitored at 550 nm by following the reduction of cytochrome c by ubiquinol. The assay was started by adding the sample to the reaction mixture (in mM: 35 K_2HPO_4, pH 7.2, 1 EDTA, 5 $MgCl_2$, 1 KCN, 5 μM rotenone) containing 15 μM cytochrome c and 15 μM ubiquinol, at 30 °C. Complex III activity was expressed in rate constant (k) per minute per milligram of protein and corrected for citrate synthase activity.

Cytochrome c oxidase assay

Complex IV activity was determined at 550 nm by measuring the oxidation of reduced cytochrome c by cytochrome c oxidase. The reduced cytochrome c was prepared by mixing its oxidized form with ascorbate and then dialysed for 24 h against a 0.01 M phosphate buffer, pH 7.0, at 4 °C. The assay was started by adding the sample to the reaction buffer (10 mM K_2HPO_4, pH 7) containing 50 μM reduced cytochrome c and 1 mM ferricyanide, at 30 °C. Complex IV activity was expressed in rate constant (k) per minute per milligram of protein and corrected for citrate synthase activity.

Citrate synthase assay

Citrate synthase (CS) activity was performed at 412 nm following the reduction of 0.2 mM 5,5′-dithio-bis(2-nitrobenzoic acid) in the presence of 0.2 mM acetyl-CoA and 0.1 mM oxaloacetate in a medium with 100 mM Tris–HCl, pH 8.0 and 0.1% Triton X-100. CS activity was expressed in nanomoles per minute per milligram of protein.

Analysis of mitochondrial membrane potential

The mitochondria membrane potential was determined by using the cationic fluorescent probe tetramethyl rhodamine methyl ester ($TMRM^+$), which accumulates predominantly in polarized mitochondria (Ward et al., 2000). Thus the variation of $TMRM^+$ retention was studied in order to estimate changes in mitochondrial membrane potential. Following a washing step with Na^+ medium containing (in mM): 135 NaCl, 5 KCl, 0.4 KH_2PO_4, 1.8 $CaCl_2$, 1 $MgSO_4$, 20 HEPES, and 5.5 glucose, pH 7.4, cells were incubated in Na^+ medium containing 150 nM $TMRM^+$ (quench mode) for 1 h at 37 °C. Basal fluorescence (540 nm excitation and 590 emission) was measured using a Microplate Spectrofluorometer Gemini EM (Molecular Devices, USA) for 5 min, followed by the addition of 1 μM FCCP and 2 μg/ml oligomycin, which produced maximal mitochondrial depolarization. Results were expressed as the difference between the increase of $TMRM^+$ fluorescence upon addition of FCCP plus oligomycin and basal fluorescence values.

Analysis of apoptotic nuclei

The nuclear morphology of HD and CTR cybrids exposed to 3-NP or STS was analyzed by fluorescence microscopy, by using a double-staining procedure with Hoechst 33342 and propidium iodide. Following a washing step with Na^+ medium, the cells were incubated with 7.5 μg/ml Hoechst 33342 and 4 μg/ml propidium iodide, in the dark, for 3 min, at room temperature. Cells were washed 3 times in Na^+ medium in order to remove extracellular dyes and further examined and scored using the Axioscope 2 Plus upright microscope (Zeiss, Jena, Germany).

Lactate dehydrogenase (LDH) measurements

The integrity of the plasma membrane was determined by monitoring the activity of the cytoplasmic enzyme LDH in the extracellular incubation medium, which represents a common procedure to determine membrane leakage and necrotic cell damage. After exposure to 3-NP or STS, the incubation medium was collected (extracellular) and the cells were lysed in 10 mM HEPES (pH 7.4) plus 0.01% Triton X-100 (intracellular) and frozen at −80 °C. Cell debris in both samples were removed by centrifugation at 14,000 rpm (Eppendorf Centrifuge 5417R), for 10 min. LDH was determined spectrophotometrically, by following the rate of conversion of reduced nicotinamide adenine dinucleotide (NADH) to oxidized NAD^+ at 340 nm (Bergmeyer and Bernt, 1974). LDH released into the extracellular medium was expressed as a percentage of the total LDH activity in the cells [% of LDH released = extracellular LDH/(extracellular LDH + intracellular LDH)].

Analysis of intracellular superoxide ions

The cybrids were incubated for 60 min at 37 °C in the presence of 5 μM DHE, in Na^+ medium. DHE is a cell-permeable fluorescent dye that, once internalized, is oxidized by superoxide to fluorescent ethidium bromide, which intercalates into DNA. DHE itself shows a blue fluorescence (355 nm excitation, 420 nm emission) in cell cytoplasm until oxidation to form ethidium, which becomes red fluorescent (518 nm excitation, 605 nm emission) upon DNA intercalation. Ethidium bromide fluorescence intensity was measured continuously for 1 h at 37 °C, and the relative level of superoxide production quantified, using a Microplate Spectrofluorometer Gemini EM (Molecular Devices, USA). At the end of each experiment, the cells were scrapped to quantify cell protein in each well, using the BioRad protein assay, and ethidium fluorescence was corrected for variations in total protein between wells. The values were normalized to the percentage of control (untreated cybrids).

Intracellular hydroperoxides analysis

Cybrids were incubated for 30 min in the presence of 20 μM $DCFH_2$-DA, a stable non-fluorescent cell permeable compound, at 37 °C in Na^+ medium, pH 7.4. When internalized by the cell, $DCFH_2$-DA is hydrolyzed to $DCFH_2$ by intracellular esterases and rapidly oxidized to the highly green fluorescent component 2,7-dichlorofluorescein (DCF) by endogenous hydroperoxides. Intracellular levels of peroxides were measured by following DCF fluorescence (480 nm excitation, 550 nm emission) at 37 °C continuously for 1 h, using a microplate reader Spectrofluorometer Gemini EM (Molecular Devices, USA). In order to correct the DCF fluorescence values for variations in total protein content in the wells, cell protein in each well was quantified by the BioRad protein assay. The values were normalized to the percentage of the control (untreated cybrids).

Caspase-3 activity assay

After washing, cells were scrapped at 4 °C in lysis buffer containing 25 mM HEPES, 2 mM $MgCl_2$, 1 mM EDTA and 1 mM EGTA, pH 7.5,

Please cite this article as: Ferreira, I.L., et al., Mitochondrial-dependent apoptosis in Huntington's disease human cybrids, Exp. Neurol. (2010), doi:10.1016/j.expneurol.2010.01.002

supplemented with 2 mM DTT, 0.1 mM phenylmethylsulphonyl fluoride (PMSF) and 1:1000 of protease inhibitor cocktail (chymostatin, pepstatin A, leupeptin and antipain). Cells were frozen two times in liquid N_2 and centrifuged at 14,000 rpm for 10 min (Eppendorf Centrifuge 5417R). The resulting supernatants were assayed for protein content by the BioRad protein assay. To measure caspase-3 activity, 30 μg protein were added to a reaction buffer [25 mM HEPES, 10% (m/v) sucrose, 0.1% (m/v) 3-[(3-cholamidopropyl) dimethylammonio]-1-propane-sulfonate CHAPS), pH 7.5] containing the colorimetric substrate (100 μM) for caspase-3 (Ac-DEVD-pNA)-like activity. The reaction mixture was incubated at 37 °C for 2 h, and the formation of pNA was measured at 405 nm using a microplate reader Spectra Max Plus 384 (Molecular Devices, USA). Caspase-like activity was calculated as the increase above control for equal amount of loaded protein.

Western blot analysis in mitochondrial and cytosolic subcellular fractions

After a washing step, cybrids were scrapped at 4 °C in sucrose buffer containing 250 mM sucrose, 20 mM HEPES, 100 mM KCl, 1.5 mM $MgCl_2$, 1 mM EDTA and 1 mM EGTA, pH7.5/KOH, supplemented with 1 mM DTT, 1 mM PMSF and 1:1000 protease cocktail inhibitor (chymostatin, pepstatin A, leupeptin and antipain). Cellular extracts were homogenized (20 strokes) and centrifuged at 500×*g* for 12 min to pellet the nucleus and cell debris. The supernatant was further centrifuged at 12,000×*g* for 20 min and the resulting pellet (mitochondrial fraction) was resuspended in supplemented TNC buffer containing 10 mM Tris acetate pH 8, 0.5% Nonidet P40, 5 mM $CaCl_2$ supplemented with 1:1000 of protease cocktail inhibitor. TCA 15% was added to the supernatant and centrifuged at 15,000×*g* for 10 min. The resulting pellet (cytosolic

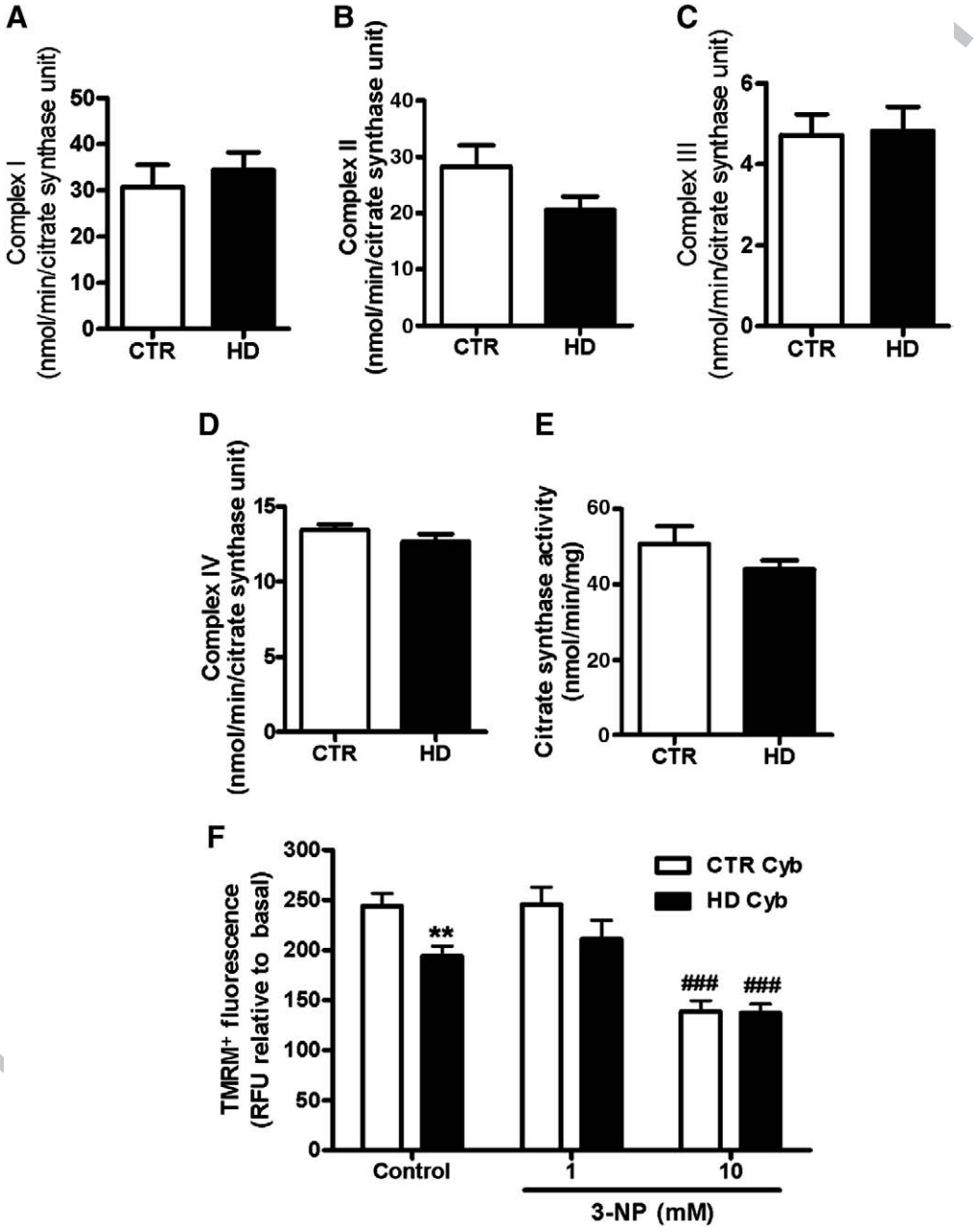

Fig. 1. Mitochondrial specific activities of complexes I-IV and mitochondrial membrane potential in HD and CTR cybrids. Mitochondrial complex enzymatic activities (A–D) normalized for the activity of citrate synthase (E) and mitochondrial membrane potential (F) were determined as described in Materials and methods. No significant differences were observed in the respiratory complexes activities. Data are the mean ± S.E.M. of 6–8 independent experiments performed in duplicates. Statistical analysis was performed by two-way ANOVA, followed by Bonferroni post test. *$p<0.05$, **$p<0.01$ when compared to CTR cybrids; $^{###}p<0.001$ when compared to control (untreated) conditions.

Please cite this article as: Ferreira, I.L., et al., Mitochondrial-dependent apoptosis in Huntington's disease human cybrids, Exp. Neurol. (2010), doi:10.1016/j.expneurol.2010.01.002

fraction) was resuspended in supplemented sucrose buffer and adjusted to pH 7 with 2.5 M KOH. Protein content was determined by BioRad method, and the samples were denaturated with 6 times concentrated denaturating buffer at 95 °C, for 5 min. Equivalent amounts of protein were separated on a 15% SDS-PAGE gel electrophoresis and electroblotted onto polyvinylidene difluoride (PVDF) membranes. The membranes were further blocked with 5% fat-free milk and incubated with antibodies directed against the denatured form of cytochrome c (Cyt c, 1:500), AIF (1.1000), Bax (1:1000), Bim (1:1000), Bak (1:5000), Bcl-2 (1:500), α-tubulin (1:20000) and mitochondrial DNA-encoded cytochrome c oxidase subunit I (COX-I, 1:500). In some membranes retaining mitochondrial samples where labeling with COX-I was not possible, we used the antibody directed against α-tubulin (1:20000) to normalize the amount of protein per lane. Tubulin is an inherent component of mitochondrial membranes (Carré et al., 2002) and its levels did not change in any of the treatments used in this study. Immunoreactive bands were visualized by alkaline phosphatase activity after incubation with ECF reagent on a BioRad Versa Doc 3000 Imaging System.

Mitochondrial DNA (mtDNA) screening

Total DNA was extracted from 5 HD and 3 CTR cybrids by using standard methods (Treco et al., 1992) and quantified by UV spectrophotometry (λ = 260 nm). Automated sequencing analysis were used, according to the manufacturer's instructions (3130 ABI Prism sequencing system), using BigDye® Terminator Ready Reaction Mix v1.1 (Applied Biosystems), for investigation of 11 mtDNA regions corresponding to nucleotides 1435-1917, 3150-3769, 4074-4703, 4886-5021, 7241-7644, 8222-8461, 8915-9413, 11720-11819, 13515-13727, 14420-14855, 15023-15450, allowing the screening of 31 confirmed pathogenic mutations, 105 reported mutations and 288 polymorphisms, including 4 haplogroup markers, according to MITOMAP (www.mitomap.org). Evolutionary conservation analysis among species for positions with novel variants identified was achieved using ENSEMBL® tools.

Statistical analysis

No significant differences in biochemical studies were observed between the HD cybrid lines and the three CTR cybrids used in this work. Therefore data were expressed as the mean ± S.E.M. of the number of experiments indicated in the figure legends. Comparisons between multiple groups were performed with a two-way analysis of variance (ANOVA), followed by Bonferroni post-test for comparison between experimental groups. Student's *t* test was also performed for comparison between two Gaussian populations, as described in figure legends. Significance was accepted at $p<0.05$.

Results

Mitochondrial electron transport chain activities and mitochondrial membrane potential

We measured the activity of mitochondrial respiratory chain complexes and the mitochondrial membrane potential in HD and CTR cybrids. Our data show no significant changes in the activities of respiratory complexes I, II, III and IV (Figs. 1A–D) or citrate synthase (Fig. 1E) in HD vs. CTR cybrids. Although the putative basal leak current and the coupling between oxygen consumption and ATP synthesis may be underestimated by assaying the catalytic activities of mitochondrial complexes, the latter measurement is important to evaluate putative changes between our HD cybrids and the data generated by Swerdlow et al. (1999).

We determined $TMRM^+$ mitochondrial accumulation after complete mitochondrial depolarization due to the addition of FCCP plus oligomycin, which gave rise to a measurable "spike" of cell fluorescence as a result of $TMRM^+$ dequenching. We observed a slight, but significant, decrease in $TMRM^+$ release from mitochondria, suggestive of decreased mitochondrial membrane potential in untreated HD cybrids (Fig. 1F). The 3-NP evoked decrease in $TMRM^+$ release was similarly exacerbated (50% decrease, $p<0.001$) upon exposure of both HD and CTR cybrids to 10 mM 3-NP, but not 1 mM 3-NP (Fig. 1F).

Mitochondrial DNA (mtDNA) screening

Despite the lack of differences in mitochondrial complexes activities, both HD and CTR cybrids were subjected for mtDNA screening. Results depicted in Table 1 summarize mtDNA findings in cybrids derived from HD patients and CTR subjects. The results were heterogeneous, revealing different patterns of mtDNA variations, both in controls and HD patients and sequence variations were found in 3 (60%) out of 5 patients. One pathogenic mutation, 3394A > G, with status "unclear," according to MITOMAP (www.mitomap.org) was found in one (HD-5) of 5 patients (20%) with 38-year-olds and 25/44 CAG repeats genotype, together with other polymorphic variants. Furthermore, we found 3 novel sequence variations in the control subjects, occurring in genetic regions that are phylogenetically moderate or highly conserved.

Effect of 3-NP and STS on cell viability

In order to evaluate the susceptibility of HD vs. CTR cybrids, we studied the effect of 3-NP and STS on nuclei morphology and LDH release. The cybrids were incubated with 1 and 10 mM 3-NP (Figs. 2A,

Table 1
Summary of mtDNA investigation in HD and control cybrids.

Sample	mtDNA sequence variations	Status (according to MITOMAP)	Gene
HD-1	None		
HD-2	None		
HD-3	3348A>G	CRP	MTND1
	11719G>A	CRP UnP in oral cancer	MTND4
	14766C>T	CRP	MTCYB
HD-4	3618T>C*	CRP	MTND1
HD-5	3394T>C	CRP; SM in acute leukaemia; PM "unclear" in LHON/NIDDM/CPT deficiency	MTND1
	4216T>C	CRP; haplogrup marker JT	MTND1
	11719G>A	CRP; UnP in oral cancer	MTND4
	13708G>A	CRP; haplogroup marker J	MTND5
	14766C>T	CRP	MTCYB
	14798T>C	CRP	MTCYB
CTR-1	7621T>C	CRP	MTCO2
	8291A>G	Novel	MTNC7
CTR-2	3348A>G	CRP	MTND1
	4172T>A	Novel	MTND1
	7566G>A*	Novel	MTTD (tRNA asp)
	11719G>A	CRP; UnP in oral cancer	MTND4
	11938C>T	CRP	MTND4
	14766C>T	CRP	MTCYB
CTR-3	3348A>G	CRP	MTND1
	4172T>A	Novel	MTND1
	7566G>A*	Novel	MTTD (tRNA asp)
	11719G>A	CRP; UnP in oral cancer	MTND4
	11938C>T	CRP	MTND4
	14766C>T	CRP	MTCYB

Note: the nomenclature of genes is presented according to MITOMAP; CRP: coding region polymorphism; *heteroplasmy; SM: somatic mutation; PM: point mutation; UnP: unpublished polymorphism; LHON: Leber hereditary optic neuropathy; NIDDM: non-insulin dependent diabetes mellitus; CPT: carnitine palmitoyl transferase.

Please cite this article as: Ferreira, I.L., et al., Mitochondrial-dependent apoptosis in Huntington's disease human cybrids, Exp. Neurol. (2010), doi:10.1016/j.expneurol.2010.01.002

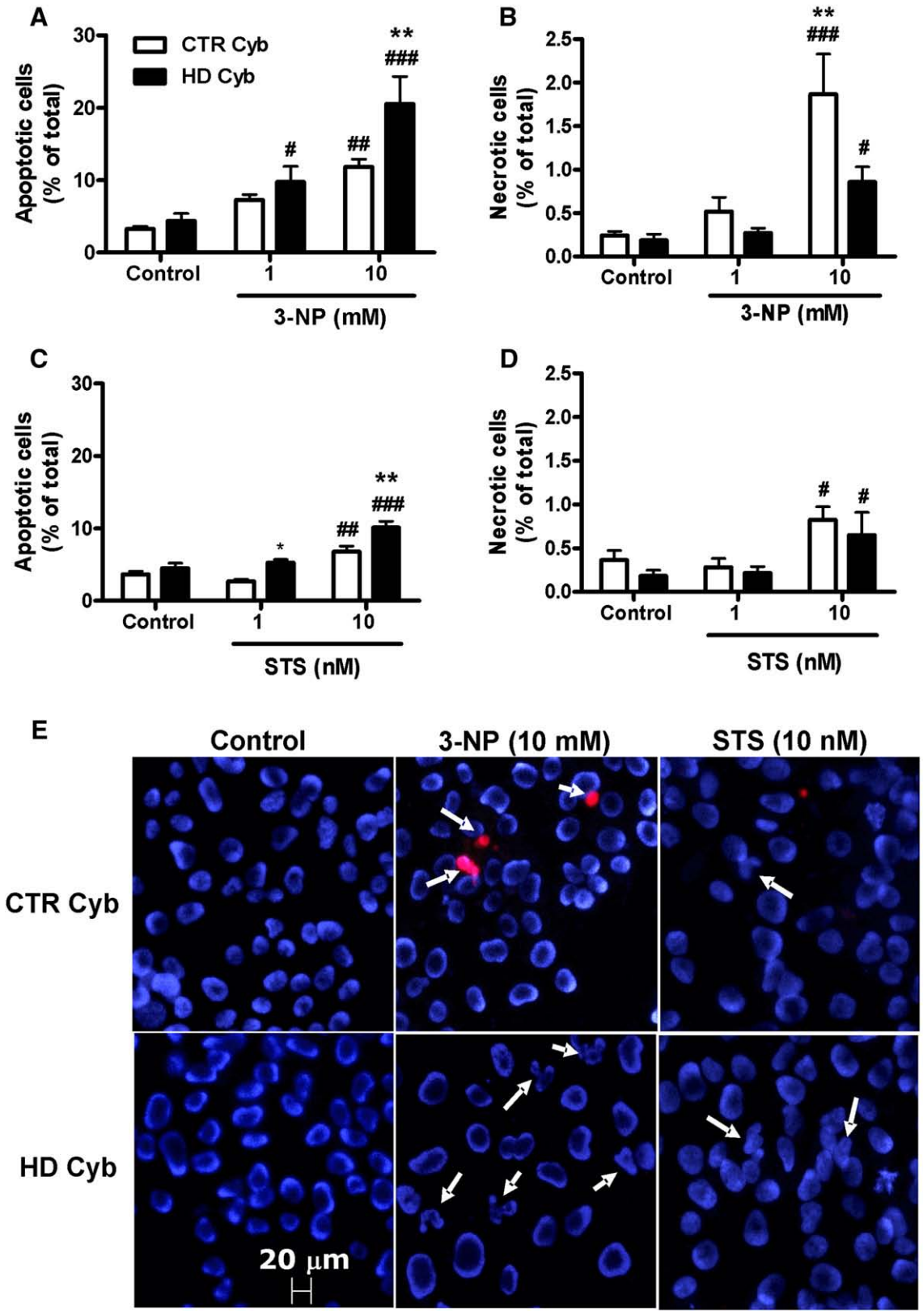

Fig. 2. Apoptotic and necrotic cell death induced by 3-NP (A, B, and E) or STS (C, D, and E) in HD and CTR cybrids. Cells cultured in glass coverslips were incubated with 3-NP (1, 10 mM) or STS (1, 10 nM) for 24 h or 15 h, respectively. At the end of the incubation the cells were incubated for 3 min with Hoechst 33342 plus propidium iodide and observed under fluorescence microscopy for nuclei morphology (200–300 cells *per* field and 3 fields *per* condition were counted). (E) shows a representative image of the cells. Data are the mean ± S.E.M. of 3 independent experiments performed in duplicates. Statistical analysis was performed by two-way ANOVA, followed by Bonferroni post test. $^{*}p<0.05$, $^{**}p<0.01$ when compared to CTR cybrids; $^{\#}p<0.05$, $^{\#\#}p<0.01$ and $^{\#\#\#}p<0.001$ when compared to control (untreated) conditions.

Please cite this article as: Ferreira, I.L., et al., Mitochondrial-dependent apoptosis in Huntington's disease human cybrids, Exp. Neurol. (2010), doi:10.1016/j.expneurol.2010.01.002

B and E) or 1 and 10 nM STS (Figs. 2C–E) and compared with non-treated cells (control). A significant number of apoptotic cells displaying condensed and/or fragmented chromatin was observed in HD cybrids incubated with 1 mM 3-NP ($p<0.05$) and 10 mM 3-NP ($p<0.001$) when compared to untreated HD cybrids (Fig. 2A). In these conditions, CTR cybrids exhibited a significant increase in the number of apoptotic cells only when incubated in the presence of 10 mM 3-NP ($p<0.01$) (Fig. 2A). For the higher 3-NP concentration tested a significant difference between HD and CTR cybrids was observed ($p<0.01$), suggesting an increased susceptibility of HD cybrids to undergo an apoptotic mode of cell death upon exposure to 3-NP (Fig. 2A). Incubation of HD and CTR cybrids with 1 mM 3-NP did not significantly affect the number of necrotic cells, compared to untreated conditions (control) (Fig. 2B). Conversely, CTR cybrids exhibited morphological characteristics of necrosis following exposure to 10 mM 3-NP, which were significantly more evident than in HD cybrids ($p<0.01$) (Fig. 2B). These results evidence a higher susceptibility of CTR cybrids to undergo a necrotic mode of cell death mode in response to 3-NP exposure. Analysis of LDH release confirmed these observations (Fig. 3A). A significant increase in LDH release was observed in both CTR and HD cybrids subjected to 10 mM 3-NP; however, CTR cybrids showed a preferential mode of necrotic cell death, as determined by a higher loss of plasma membrane integrity (Fig. 3A).

We also tested the effect of STS on apoptotic and necrotic nuclei morphology on both HD and CTR cybrids (Figs. 2C–E). Our results show that 1 nM STS produced a small, but significant, increase in the number of HD cybrids undergoing apoptosis, compared with CTR cybrids ($p<0.05$) (Fig. 2C). This effect was more pronounced in the presence of 10 nM STS, since both CTR ($p<0.01$) and HD cybrids ($p<0.001$) showed a higher number of apoptotic nuclei compared to untreated cybrids (control) (Figs. 2C and E). Under these conditions, HD cybrids were more susceptible to apoptosis induced by 10 nM STS compared to CTR cybrids ($p<0.01$). In cells exposed to 10 nM STS, we also observed a small increase in the number of necrotic cells, when compared to untreated conditions (control) ($p<0.05$), but no differences were observed between HD and CTR cybrids (Fig. 2D). However, no significant differences caused by STS (1 or 10 nM) were observed on LDH release in both CTR and HD cybrids (Fig. 3B).

These results show that HD cybrids exhibit morphological characteristics of apoptosis following 3-NP or STS treatment, being the HD cybrids more susceptible to apoptosis compared with CTR cybrids. Conversely, upon 3-NP exposure, CTR cybrids appear to preferentially undergo a necrotic mode of cell death, whereas incubation with STS does not differentially affect necrotic cell death in HD and CTR cybrids.

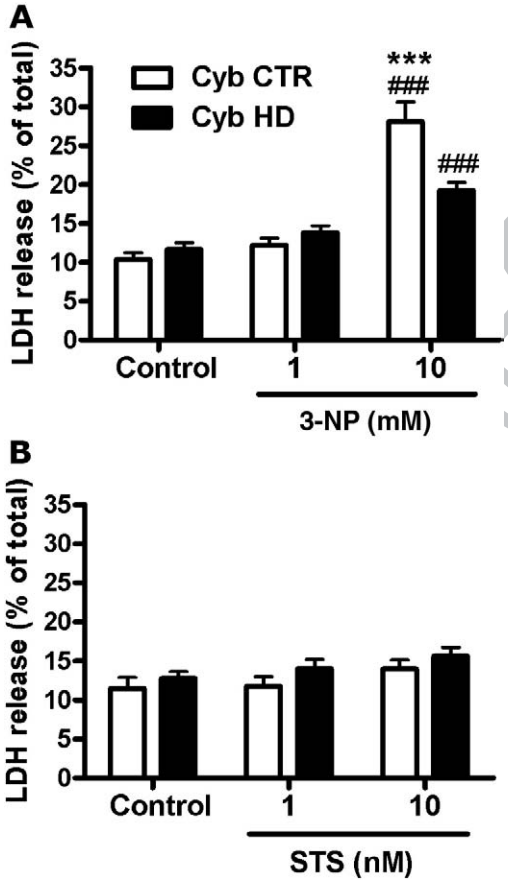

Fig. 3. Effect of 3-NP (A) or STS (B) on LDH release in HD and CTR cybrids. Cells were incubated in the absence or in the presence of 3-NP (1, 10 mM) or STS (1, 10 nM) for 24 h or 15 h, respectively, and LDH was determined spectrophotometrically as described in the Material and Methods. Data are the mean ± S.E.M. of 4–8 independent experiments performed in duplicates. Statistical analysis was performed by two-way ANOVA, followed by Bonferroni post test. ***$p<0.001$ when compared to HD cybrids and ###$p<0.001$ when compared to control (untreated) conditions.

Effect of 3-NP and STS on reactive oxygen species production

To explain the higher susceptibility of HD cybrids when exposed to toxic stimuli, we examined the production of endogenous reactive oxygen species (ROS). For this purpose, HD or CTR cybrids were incubated in the absence or presence of 3-NP or STS and the levels of superoxide ions and hydroperoxides were analyzed by measuring ethidium or DCF fluorescence, respectively.

Our results show no differences on superoxide levels between HD and CTR cybrids under basal conditions (untreated HD vs. CTR cybrids) (Fig. 4A). However, superoxide production increased in HD cybrids upon exposure to 3-NP (0.1–10 mM), compared with untreated conditions (control) (Fig. 4B). A significant difference in superoxide production in HD compared to CTR cybrids was only observed for the higher concentration of 3-NP tested (10 mM) ($p<0.05$). Incubation with STS (0.1–10 nM) caused a significant increase in superoxide production in HD cybrids, as compared to CTR or untreated cybrids. Similarly to 3-NP, exposure to STS did not affect the levels of superoxide in CTR cybrids (Fig. 4C).

By measuring DCF fluorescence we demonstrate that under basal conditions HD cybrids are endowed with a significant higher amount of hydroperoxides production, compared to CTR cybrids ($p<0.01$) (Fig. 4D); however, no differences between HD and CTR cybrids were observed when the cells were subjected to increasing concentrations of 3-NP (Fig. 4E). Incubation with 10 mM 3-NP increased hydroperoxides production, in HD and CTR cybrids, compared to untreated conditions (control) ($p<0.001$) (Fig. 4E). Incubation with STS produced a dose-dependent increase in hydroperoxides production in HD cybrids compared to untreated conditions (control) and CTR cybrids (Fig. 4F), suggesting that HD cybrids are more susceptible to STS-induced hydroperoxide production. A significant increase in hydroperoxide production in CTR cybrids was only observed in the presence of the highest concentration of STS tested (10 nM) ($p<0.01$).

Effect of 3-NP and STS on caspase-3 activation

Since HD cybrids exhibited a higher percentage of cells displaying apoptotic morphology (as determined in Fig. 2), we also investigated the effect of 3-NP and STS on caspase-3 activation in both CTR and HD cybrids (Figs. 5A and B). Although no significant changes were observed in CTR cybrids subjected to mitochondrial inhibition, treatment with 10 mM 3-NP was effective in inducing caspase-3-like activity in HD cybrids, when compared to untreated cybrids (control) ($p<0.001$) or with CTR cybrids ($p<0.01$) (Fig. 5A). STS incubation also caused a significant increase in caspase-3 activity in

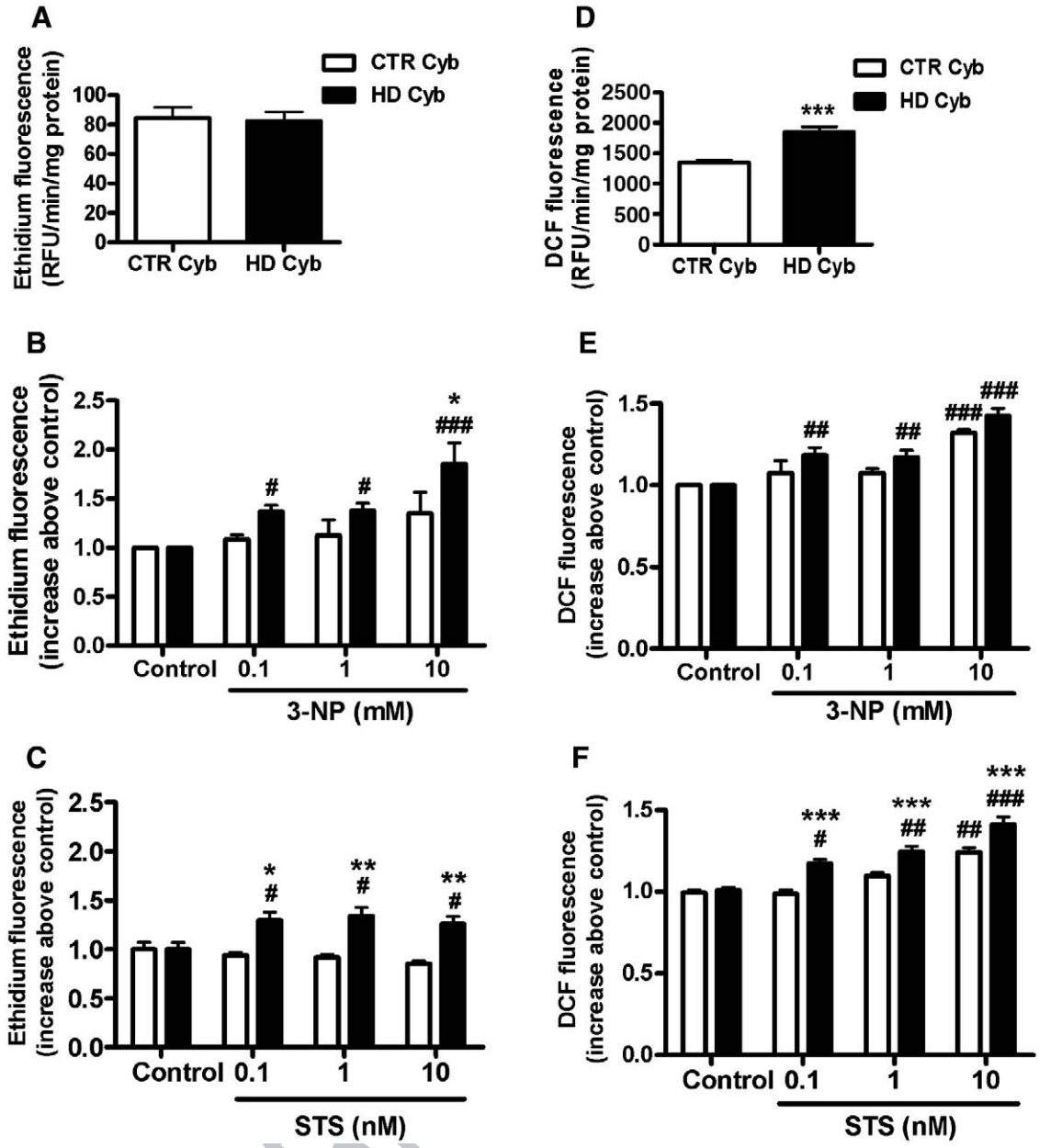

Fig. 4. ROS production in HD and CTR cybrids. Cells were incubated in the absence or in the presence of 3-NP (0.1, 1 and 10 mM) or STS (0.1, 1 or 10 nM) for 24 h or 15 h, respectively. The relative levels of superoxide ions (A, B and C) were determined following ethidium fluorescence after a pre-incubation with 5 μM DHE for 1 h, and the levels of hydroperoxides (D, E and F) were measured following DCF fluorescence after a 30 min incubation with 20 μM $DCFH_2$-DA. Results are expressed as the mean ± S.E.M. from 3 independent experiments. Statistical analysis was performed by two-way ANOVA, followed by Bonferroni post test. $^{*}p<0.05$, $^{**}p<0.01$ and $^{***}p<0.001$ when compared to CTR cybrids and $^{\#}p<0.05$, $^{\#\#}p<0.01$, $^{\#\#\#}p<0.001$ when compared to control (untreated) conditions.

HD cybrids in the presence of the highest (10 nM) concentration of STS tested, when compared to control conditions (untreated HD cybrids) ($p<0.01$) (Fig. 5B). However, we did not observe significant differences in the susceptibility of HD cybrids compared to CTR cybrids when examining caspase-3 activity in response to STS (Fig. 5B), despite the observation of a significant number of apoptotic nuclei in these conditions (Fig. 2C). These data were confirmed by α-spectrin cleavage into 150 and 120 kDa fragments, induced by 3-NP or STS exposure (data not shown).

Effect of 3-NP on pro-apoptotic Cyt c, AIF, Bax, Bak, and Bim, and anti-apoptotic Bcl-2 protein levels

Because cell death, including DNA fragmentation, caspase-3-like activation and superoxide production were more evident in HD cybrids exposed to 3-NP, we characterized in more detail the levels of pro- and anti-apoptotic proteins involved in 3-NP-induced apoptosis in this model. The levels of both mitochondrial and cytosolic cytochrome c, Bax and Bcl-2 and mitochondrial Bak, Bim and AIF were analyzed by western blotting in HD and CTR cybrids (Fig. 6). Cytochrome c was released in a significant manner from mitochondria of HD cybrids subjected to 10 mM 3-NP, when compared to both untreated HD cybrids (control) ($p<0.05$) or CTR cybrids ($p<0.01$) (Fig. 6A). Interestingly, when statistical analysis was performed by unpaired Student's *t* test in control conditions, a significant increase in cytochrome c in cytosol of HD vs. CTR cybrids was also detected ($p<0.05$). Slight changes in cytochrome c release under basal conditions seem to correlate with a small decrease in mitochondrial membrane potential. AIF, which induces apoptotic cell death through a caspase-independent pathway, was released in a similar manner

Please cite this article as: Ferreira, I.L., et al., Mitochondrial-dependent apoptosis in Huntington's disease human cybrids, Exp. Neurol. (2010), doi:10.1016/j.expneurol.2010.01.002

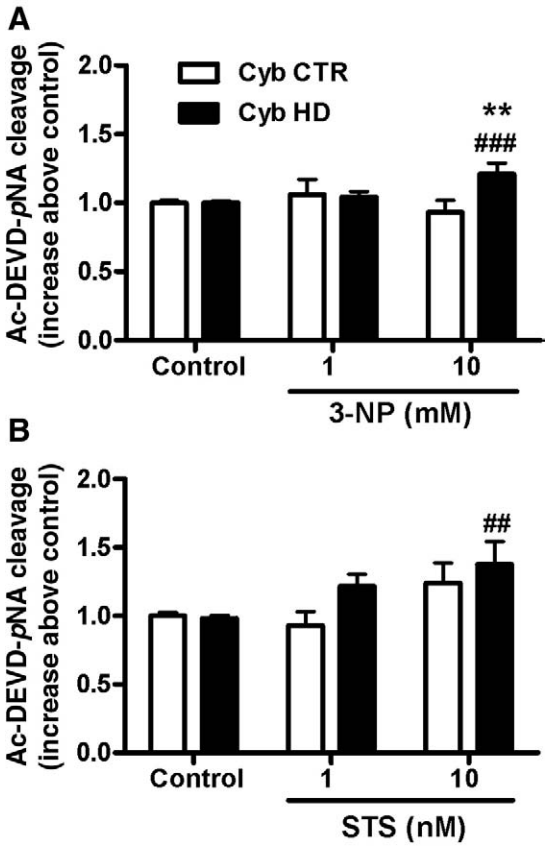

Fig. 5. Caspase-3 activation induced by 3-NP (A) or STS (B) in HD and CTR cybrids. Cells were incubated in the absence or in the presence of 3-NP (1 and 10 mM) or STS (1 or 10 nM) for 24 h and 15 h, respectively. Caspase-3-like activity was measured by following the cleavage of the colorimetric substrate Ac-DEVD-*p*NA. The activity is expressed as the increase in optic density values above the control (untreated cybrids). Results are expressed as the mean ± S.E.M. from 10–12 independent experiments performed in duplicates. Statistical analysis was performed by two-way ANOVA, followed by Bonferroni post test. $^{**}p<0.01$ when compared to CTR cybrids; $^{\#\#}p<0.01$, $^{\#\#\#}p<0.001$ when compared to control (untreated) conditions.

from HD and CTR cybrids mitochondria upon exposure to 3-NP (Fig. 6B). The pro-apoptotic protein Bim was present in higher amounts in mitochondria derived from non-treated (control) HD, compared to CTR, cybrids ($p<0.01$ analyzed by *t* test), but exposure to 3-NP did not highly affect Bim expression in HD cybrids (Fig. 6C). Interestingly, for the highest concentration of 3-NP tested (10 mM), CTR cybrids showed a significant increase in Bim levels in the mitochondria when compared to untreated conditions (control) ($p<0.05$) or with HD cybrids exposed to 3-NP ($p<0.001$) (Fig. 6C). Incubation with 3-NP did not significantly affect the levels of the proapoptotic protein Bak in mitochondria from both HD and CTR cybrids. However, our results demonstrate that under basal conditions (untreated cybrids) the levels of Bak are higher in HD than in CTR cybrids ($p<0.05$) (Fig. 6D). Treatment with 3-NP (1 and 10 mM) increased the translocation of Bax from the cytosol to the mitochondria in both CTR and HD cybrids ($p<0.05$); however, no significant differences were observed between HD and CTR cybrids (Fig. 6E). Finally, cytosolic or mitochondrial levels of the anti-apoptotic protein Bcl-2 were unaffected under basal or 3-NP-treated conditions in both HD and CTR cybrids (Fig. 6F).

Discussion

Mitochondria are central in the process of apoptosis, a mechanism leading to neuronal loss in neurodegenerative disorders like HD (Kroemer and Reed, 2000; Beal, 2005; García-Martínez et al., 2007; Yang et al., 2008). In the present study we provide evidence that human HD cybrids show subtle mitochondrial modifications. Indeed, HD cybrids are more susceptible than CTR cybrids to mitochondrial-dependent cell degeneration produced by the mitochondrial complex II inhibitor 3-NP and the classic apoptotic inducer STS. In HD cybrids, treatment with 3-NP caused the release of mitochondrial cytochrome c, the subsequent activation of caspase-3, as well as the release of mitochondrial AIF. This effect appears to be mediated by mitochondrial translocation of Bax. Moreover, increased mitochondrial levels of Bim and Bak, a slight decrease in mitochondrial membrane potential concomitant with the release of cytochrome c, and increased hydroperoxide production in non-treated HD cybrids may explain the increased susceptibility to apoptosis caused by exposure to stress inducers (3-NP or STS). Conversely, CTR cybrids are more vulnerable to necrotic cell death upon 3-NP treatment, and no changes in caspase-3 activation are observed. Increased mitochondrial Bax, and particularly Bim, may contribute to promote a different mode of cell death in 3-NP treated-CTR cybrids.

Previous evidence showed that both nuclear and mitochondrial genomes are damaged in the 3-NP chemically induced HD mouse model and in the HD R6/2 transgenic mice (Acevedo-Torres et al., 2009). Lymphocytes from HD patients have higher frequencies of mtDNA deletions and oxidative stress, suggesting that CAG repeat instability, and thus mutant huntingtin, are a causative factor in mtDNA damage (Banoei et al., 2007). Moreover, decreased mtDNA content was correlated with the length of CAG repeats in leukocytes from HD patients (Liu et al., 2008). Data presented in Table 1 suggest that the mtDNA sequence variations are not causal for HD in the patients included in the present study, since some are also found in CTR cybrids. Additionally, there is no information regarding the CAG repeat genotype in the HD gene of CTR subjects, and thus we cannot exclude that they may be carriers for the intermediate or expanded allele and that they may develop any type of neurodegenerative disease later in life, including dementia. The presence of mtDNA variations, including an 8656A > G variant in one patient, was recently shown in a screening study for mutations in the *tRNA(leu/lys)* and *MTATP6* genes of 20 patients with HD (Kasraie et al., 2008). However, the nucleotides 8915-9207 of the same gene do not present any sequence variation in our study. Table 1 also presents one HD cybrid line carrying the 3394T > C mutation with status "unclear," previously described in cases suffering from Leber Hereditary Optic Neuropathy (LHON), which was shown to be related with HD features (Morimoto et al., 2004). Despite these observations, we cannot exclude that other genes outside the regions investigated may be involved in the disease or that mtDNA involvement is either related to deletion events or copy number alterations.

Unchanged mtDNA sequence variations correlate with the fact that no mitochondrial respiratory chain defects were found in HD, compared to CTR cybrids. These results are in agreement with previous data showing no substantial modifications in mitochondrial complexes activity in cybrid cell lines containing mtDNA from HD patients (Swerdlow et al., 1999). Furthermore, there were no significant changes in the activity of mitochondrial respiratory complexes (I–IV) or in superoxide formation among the six HD cybrid lines used in the current study. Thus, our data suggest that other mitochondrial modifications induced by full-length and/or fragments of mutant huntingtin, such as protein post-translational modifications, are retained in HD cybrids, which may be related with an interaction of mutant huntingtin with the organelle in HD carriers platelets. However, we could not detect huntingtin associated with the mitochondrial fractions derived from HD cybrids, as detected by western blotting using the anti-huntingtin antibody MAB2166 (Chemicon) (data not shown). Although HD cybrids do not express mutant huntingtin and thus cannot be directly compared with models expressing mutant huntingtin, in striatal cell lines expressing full-length mutant huntingtin (derived from knock-in mice) no significant effects on respiratory complexes activities were observed either (Milakovic and Johnson, 2005).

Please cite this article as: Ferreira, I.L., et al., Mitochondrial-dependent apoptosis in Huntington's disease human cybrids, Exp. Neurol. (2010), doi:10.1016/j.expneurol.2010.01.002

Mitochondrial dysfunction has been frequently associated with increased generation of ROS, promoting intracellular oxidative stress and leading to protein, lipid and DNA oxidation. Indeed, oxidative damage was shown to play an important role in the pathogenesis and progression of HD in the R6/2 transgenic mouse model (Perluigi et al., 2005) and also in post-mortem samples obtained from the striatum and cortex of human HD brain (Sorolla et al., 2008). Our data also demonstrate that, under basal conditions, HD cybrids are endowed with a significant higher production of hydroperoxides when compared to CTR cybrids. These data differ from a previous study showing no evidence of ROS generation, as measured with $DCFH_2$-DA in untreated HD cybrids (Swerdlow et al., 1999); however, these authors did not exclude a subtle mitochondrial pathology in these cells. In agreement, we show that HD cybrids are more vulnerable than CTR cybrids to produce superoxide upon 3-NP or STS treatment, whereas increased hydroperoxide production was mainly evoked by STS, suggesting that the presence of higher amounts of hydroperoxides in untreated HD cybrids masks the effect caused by 3-NP-induced mitochondrial inhibition.

The mitochondrial toxin 3-NP was shown to cause energy deficiency and cell death by necrosis and apoptosis in striatal, cortical and hippocampal cells (Behrens et al., 1995; Pang and Geddes, 1997; Almeida et al., 2004, 2006; Ruan et al., 2004; Brouillet et al., 2005), and both processes of cell damage have been proven to involve mitochondria (Kroemer and Reed, 2000). In the present work, exposure of HD cybrid cell lines to 3-NP or STS caused DNA fragmentation and moderate caspase-3 activation, evidencing an increased susceptibility of HD cybrids to apoptosis. However, 3-NP treated CTR cybrids died predominantly by necrosis, not involving caspase-3 activation. Recent data obtained in our laboratory using the same cybrid lines also showed that endogenous levels of ATP are higher in HD cybrids compared to CTR cybrids (author's unpublished data). Preserved ATP levels in HD cybrids may explain the preferential mode of cell death by apoptosis.

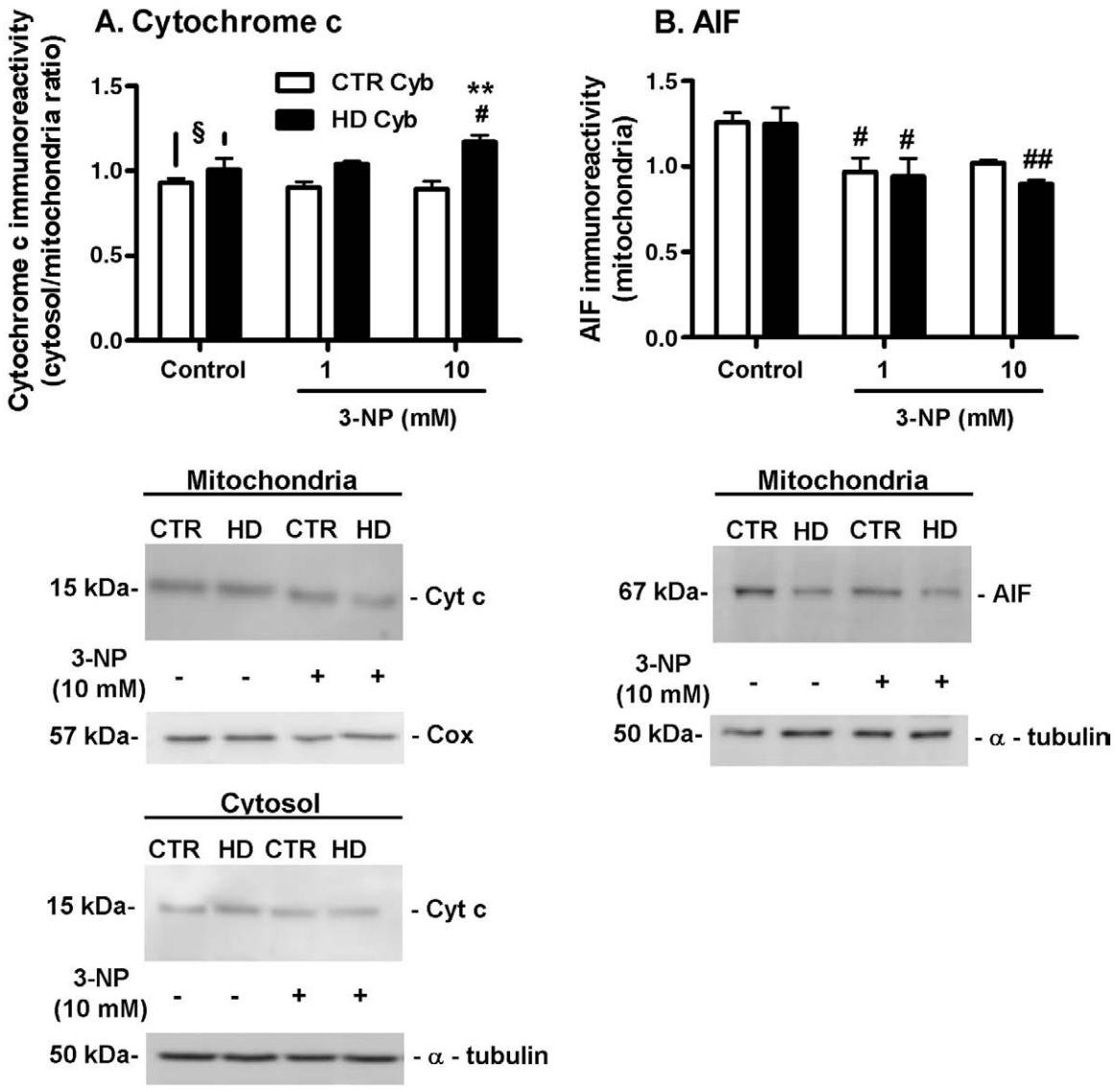

Fig. 6. Changes in cytosolic and mitochondrial levels of cytochrome c, AIF, Bax, Bim, Bak, and Bcl-2 in HD and CTR cybrids. Cells were incubated in the absence or in the presence of 3-NP (1 and 10 mM) for 24 h. Cytosolic and mitochondrial fractions were obtained as described in the Material and Methods and cytochrome c (A), AIF (B), Bim (C), Bak (D), Bax (E), and Bcl-2 (F) protein levels were analyzed by Western blotting. α-Tubulin or Cox1 were used as loading controls for analysis of cytosolic or mitochondrial fractions, respectively. The results are expressed as the mean ± S.E.M. from 3–10 independent experiments. Statistical analysis was performed by two-way ANOVA, followed by Bonferroni post test. $^{**}p<0.01$ and $^{***}p<0.001$ when compared to CTR cybrids; $^{\#}p<0.05$, $^{\#\#}p<0.01$ when compared to control (untreated) conditions. $^{\S}p<0.05$ and $^{\S\S}p<0.01$ when the HD cybrids were compared with CTR cybrids under control (untreated) conditions, and statistical analysis was performed by using Student's *t* test.

Please cite this article as: Ferreira, I.L., et al., Mitochondrial-dependent apoptosis in Huntington's disease human cybrids, Exp. Neurol. (2010), doi:10.1016/j.expneurol.2010.01.002

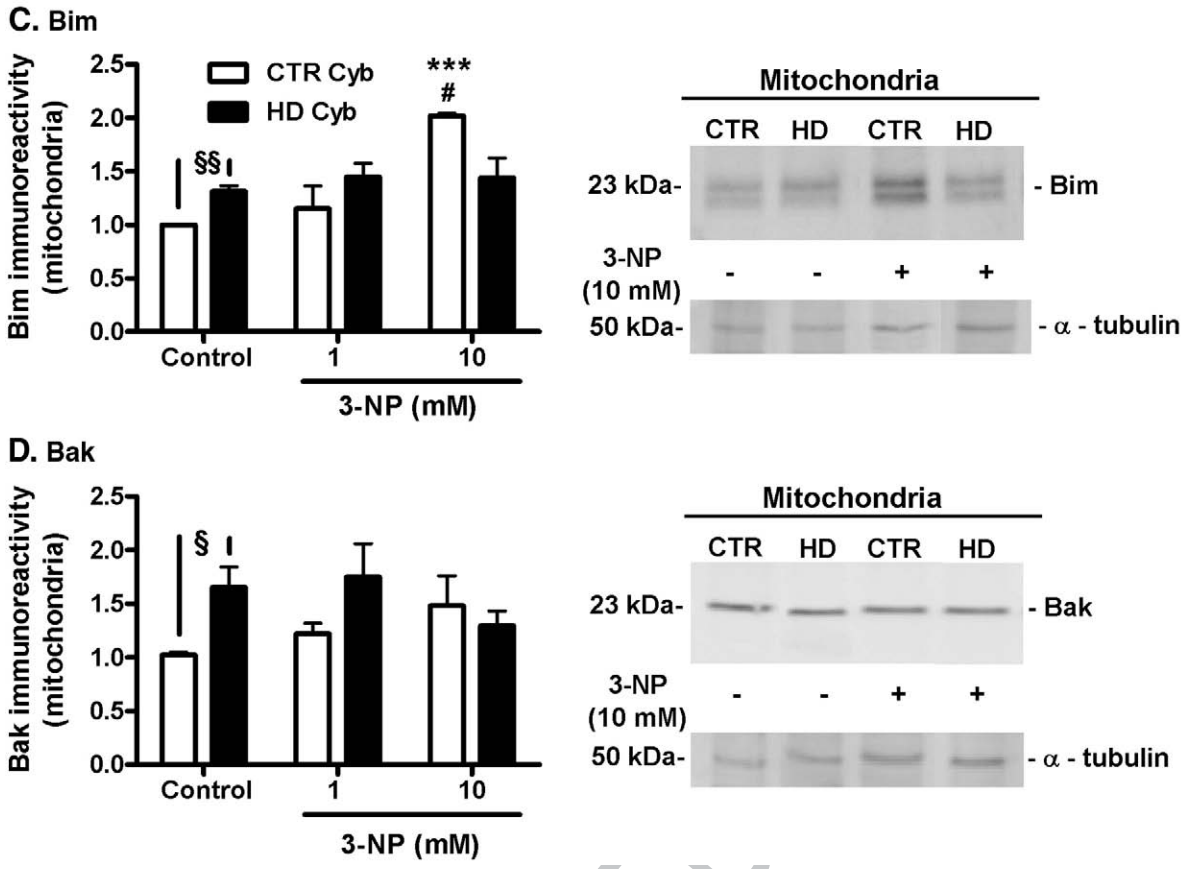

Mutant huntingtin interaction with the mitochondria, as previously observed in neuronal mitochondrial membranes of YAC72 transgenic mice (Panov et al., 2002), may cause mitochondrial abnormalities leading to cytochrome c release, and a decrease in mitochondrial membrane potential. These authors also observed that defects in mitochondrial calcium handling in HD brain mitochondria may underlie HD pathology. Similar effects were observed by us in YAC128 HD striatal neurons upon excitotoxic stimuli (Oliveira et al., 2006). However data presented by Swerdlow et al., 1999, showed no differences in CCCP-evoked cytosolic calcium between HD and CTR cybrids, suggesting equivalent mitochondrial calcium handling.

We have recently reported that 3-NP causes mitochondrial-dependent apoptotic neuronal death through the release of cytochrome c and consequent activation of caspases, or the release of AIF in cortical neurons (Almeida et al., 2004, 2006, 2009). Our present data demonstrate an increase in cytochrome c and AIF release from mitochondria, the translocation of the pro-apoptotic protein Bax to mitochondria, but no changes on the levels of Bak or the anti-apoptotic protein Bcl-2 in HD cybrids exposed to 3-NP. These data appear to be consistent with possible subtle effects of mutant huntingtin in the mitochondria of HD cybrids. Indeed, mutant huntingtin fragments were previously shown to directly induce the opening of the mitochondrial permeability transition pore in isolated mouse liver mitochondria, with the consequent release of cytochrome c (Choo et al., 2004) which leads to caspase cascade activation. Myoblasts obtained from presymptomatic and symptomatic HD subjects also show mitochondrial depolarization, cytochrome c release and increased activities of caspases 3, 8 and 9 (Ciammola et al., 2006). Increased Bax expression in B and T lymphocytes, and monocytes from HD patients, but no alterations in Bcl-2 expression levels were also recently observed by us in blood samples from HD patients (Almeida et al., 2008). Moreover, it was recently shown that Bax and Bak can mediate apoptosis without discernable association with the putative BH3-only activators (Bim, Bid and Puma) (Willis et al., 2007). Interestingly, and consistently with moderate sustained modifications of mitochondrial function in HD cybrids, non-treated HD cells showed moderate levels of cytosolic cytochrome c and increased mitochondrial levels of both Bim and Bak. It was previously shown that cell death induction by Bim(S) can occur independently of anti-apoptotic Bcl-2 protein binding, but requires Bim (S) mitochondrial targeting (Weber et al., 2007). In the R6/1 mouse model of HD, increased levels of Bim and Bid were observed at later stages of the disease (García-Martínez et al., 2007). Moreover, constitutive expression of the transgene Tet/HD94 mice resulted in increased levels of Bim and Bid proteins, but only the Bid protein returned to wild-type levels 5 months after mutant huntingtin shutdown (García-Martínez et al., 2007).

Our results suggest that mtDNA sequence variation is not a primary contributor to the development of HD pathology. Thus we hypothesize that HD cybrids may retain abnormal mitochondria from the symptomatic HD patient platelets. Indeed, both caspase-dependent and independent cell damage occurs in HD cybrids in response to 3-NP exposure, reflecting subtle modifications in mitochondria from HD patients. These alterations are considerably less than those observed in cybrid lines obtained from sporadic forms of Parkinson's (Esteves et al., 2008) and Alzheimer's (Cardoso et al., 2004) disease. Nevertheless, this *ex vivo* human mitochondrial HD model appears to be useful for studying mitochondrial-dependent defects and elucidate cell death mechanisms induced by toxic stimuli in a sub-population of HD patients. Moreover, the HD cybrids may be valuable for testing pharmacological compounds associated with improved mitochondrial function.

Acknowledgments

The authors thank the patients and families who generously contributed to this study. We also thank Dr. Isabel Nunes (Center for Neuroscience and Cell Biology, University of Coimbra) for expert

Please cite this article as: Ferreira, I.L., et al., Mitochondrial-dependent apoptosis in Huntington's disease human cybrids, Exp. Neurol. (2010), doi:10.1016/j.expneurol.2010.01.002

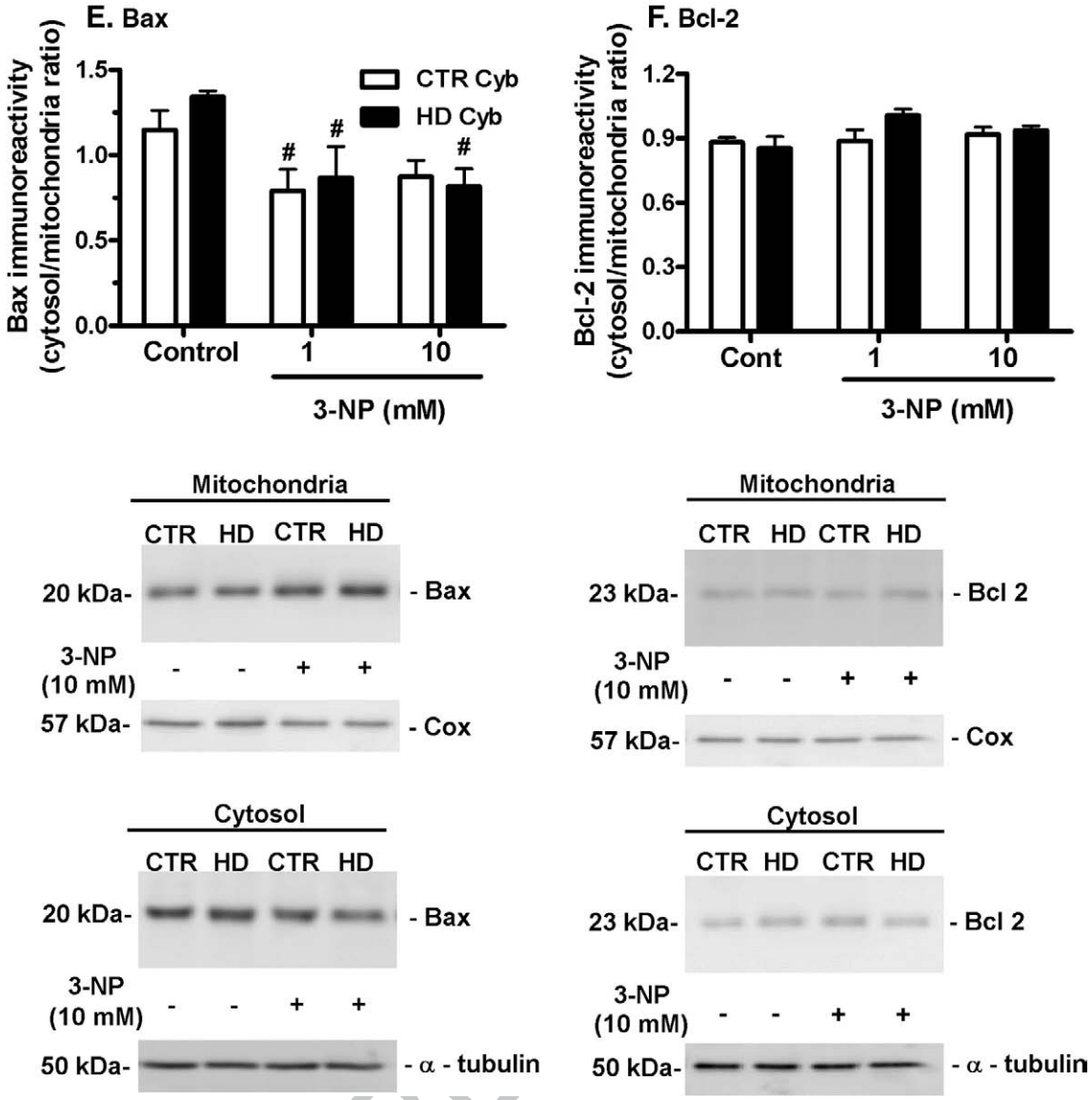

Fig. 6 (*continued*).

technical assistance with cell culture maintenance, and Dr. Russell H. Swerdlow (University of Virginia, Charlottesville, VA, USA) for the gift of ρ° NT2 cells. This work was supported by Project III/BIO/49/2005 (Instituto de Investigação Interdisciplinar, III, Universidade de Coimbra, Portugal), Project STARTER S-09 (Gabinete de Apoio à Investigação, GAI, Faculdade de Medicina, Universidade de Coimbra) and Project POCI/SAU-NEU/57310/2004 (Fundação para a Ciência e a Tecnologia, Portugal).

References

Acevedo-Torres, K., Berríos, L., Rosario, N., Dufault, V., Skatchkov, S., Eaton, M.J., Torres-Ramos, C.A., Ayala-Torres, S., 2009. Mitochondrial DNA damage is a hallmark of chemically induced and the R6/2 transgenic model of Huntington's disease. DNA Repair 8, 126–136.

Almeida, S., Domingues, A., Rodrigues, L., Oliveira, C.R., Rego, A.C., 2004. FK506 prevents mitochondrial-dependent apoptotic cell death induced by 3-nitropropionic acid in rat primary cortical cultures. Neurobiol. Dis. 17, 435–444.

Almeida, S., Brett, A.C., Góis, I.N., Oliveira, C.R., Rego, A.C., 2006. Caspase-dependent and -independent cell death induced by 3-nitropropionic acid in rat cortical neurons. J. Cell Biochem. 98, 93–101.

Almeida, S., Sarmento-Ribeiro, A.B., Januário, C., Rego, A.C., Oliveira, C.R., 2008. Evidence of apoptosis and mitochondrial abnormalities in peripheral blood cells of Huntington's disease patients. Biochem. Biophys. Res. Commun. 374, 599–603.

Almeida, S., Laço, M., Cunha-Oliveira, T., Oliveira, C.R., Rego, A.C., 2009. BDNF regulates BIM expression levels in 3-nitropropionic acid-treated cortical neurons. Neurobiol. Dis. 35, 448–456.

Aronin, N., Chase, K., Young, C., Sapp, E., Schwarz, C., Matta, N., Kornreich, R., Landwehrmeyer, B., Bird, E., Beal, M.F., Vonsattel, J.P., Smith, T., Carraway, R., Boyce, F.M., Young, A.B., Penney, J.B., DiFiglia, M., 1995. CAG expansion affects the expression of mutant huntingtin in the Huntington's disease brain. Neuron 15, 1193–1201.

Banoei, M.M., Houshmand, M., Panahi, M.S.S., Shariati, P., Rostami, M., 2007. Huntington's disease and mitochondrial DNA deletions: Event or regular mechanism for mutant huntingtin protein and CAG repeats expansion?! Cell Mol. Neurobiol. 27, 867–875.

Beal, M.F., 2005. Mitochondria take center stage in aging and neurodegeneration. Ann. Neurol. 58, 495–505.

Behrens, M.I., Koh, J., Canzoniero, L.M., Sensi, S.L., Csernansky, C.A., Choi, D.W., 1995. 3-Nitropropionic acid induces apoptosis in cultured striatal and cortical neurons. Neuroreport 6, 545–548.

Bergmeyer, H.U., Bernt, E., 1974. UV-assay with pyruvate and NADH. Methods of enzymatic analysis. Academic press, New York, pp. 574–579.

Bezprozvanny, I., Hayden, M.R., 2004. Deranged neuronal calcium signaling and Huntington disease. Biochem. Biophy. Res. Comm. 322, 1310–1317.

Bossy-Wetzel, E., Petrilli, A., Knott, A.B., 2008. Mutant huntingtin and mitochondrial dysfunction. Trends Neurosci. 31, 609–616.

Brouillet, E., Guyot, M.C., Mittoux, V., Altairac, S., Condé, F., Palfi, S., Hantraye, P., 1998. Partial inhibition of brain succinate dehydrogenase by 3-nitropropionic acid is sufficient to initiate striatal degeneration in rat. J. Neurochem. 70, 794–804.

Brouillet, E., Jacquard, C., Bizat, N., Blum, D., 2005. 3-Nitropropionic acid: a mitochondrial toxin to uncover physiopathological mechanisms underlying striatal degeneration in Huntington's disease. J. Neurochem. 95, 1521–1540.

Please cite this article as: Ferreira, I.L., et al., Mitochondrial-dependent apoptosis in Huntington's disease human cybrids, Exp. Neurol. (2010), doi:10.1016/j.expneurol.2010.01.002

Cardoso, S.M., Santana, I., Swerdlow, R.H., Oliveira, C.R., 2004. Mitochondria dysfunction of Alzheimer's disease cybrids enhances Abeta toxicity. J. Neurochem. 89, 1417–1426.

Carré, M., André, N., Carles, G., Borghi, H., Brichese, L., Briand, C., Braguer, D., 2002. Tubulin is an inherent component of mitochondrial membranes that interacts with the voltage-dependent anion channel. J. Biol. Chem. 277, 33664–33679.

Choo, Y.S., Johnson, G.V., MacDonald, M., Detloff, P.J., Lesort, M., 2004. Mutant huntingtin directly increases susceptibility of mitochondria to the calcium-induced permeability transition and cytochrome c release. Hum. Mol. Genet. 13, 1407–1420.

Ciammola, A., Sassone, J., Alberti, L., Meola, G., Mancinelli, E., Russo, M.A., Squitieri, F., Silani, V., 2006. Increased apoptosis, Huntingtin inclusions and altered differentiation in muscle cell cultures from Huntington's disease subjects. Cell Death Differ. 13, 2068–2078.

del Hoyo, P., García-Redondo, A., de Bustos, F., Molina, J.A., Sayed, Y., Alonso-Navarro, H., Caballero, L., Arenas, J., Jiménez-Jiménez, F.J., 2006. Oxidative stress in skin fibroblasts cultures of patients with Huntington's disease. Neurochem. Res. 31, 1103–1109.

Esteves, A.R., Domingues, A.F., Ferreira, I.L., Januário, C., Swerdlow, R.H., Oliveira, C.R., Cardoso, S.M., 2008. Mitochondrial function in Parkinson's disease cybrids containing an nt2 neuron-like nuclear background. Mitochondrion 8, 219–228.

Fan, M.M.Y., Raymond, L.A., 2007. *N*-methyl-D-aspartate (NMDA) receptor function and excitotoxicity in Huntington's disease. Prog. Neurobiol. 81, 272–293.

García-Martínez, J.M., Pérez-Navarro, E., Xifró, X., Canals, J.M., Díaz-Hernández, M., Trioulier, Y., Brouillet, E., Lucas, J.J., Alberch, J., 2007. BH3-only proteins Bid and Bim (EL) are differentially involved in neuronal dysfunction in mouse models of Huntington's disease. J. Neurosci. Res. 85, 2756–2769.

Gil, J.M., Rego, A.C., 2008. Mechanisms of neurodegeneration in Huntington's disease. Eur. J. Neurosci. 27, 2803–2820.

Grazina, M., Pratas, J., Silva, F., Oliveira, S., Santana, I., Oliveira, C., 2006. Genetic basis of Alzheimer's dementia: role of mtDNA mutations. Genes Brain Behav. 5 (S2), 92–107.

Huntington Study Group, 1996. Unified Huntington's Disease Rating Scale: reliability and consistency. Mov. Disord. 11, 136–142.

Kasraie, S., Houshmand, M., Banoei, M.M., Ahari, S.E., Panahi, M.S., Shariati, P., Bahar, M., Moin, M., 2008. Investigation of tRNA(Leu/Lys) and ATPase 6 Genes Mutations in Huntington's Disease. Cell. Mol. Neurobiol. 28, 933–938.

Kuhn, A., Goldstein, D.R., Hodges, A., Strand, A.D., Sengstag, T., Kooperberg, C., Becanovic, K., Pouladi, M.A., Sathasivam, K., Cha, J.H., Hannan, A.J., Hayden, M.R., Leavitt, B.R., Dunnett, S.B., Ferrante, R.J., Albin, R., Shelbourne, P., Delorenzi, M., Augood, S.J., Faull, R.L., Olson, J.M., Bates, G.P., Jones, L., Luthi-Carter, R., 2007. Mutant huntingtin's effects on striatal gene expression in mice recapitulate changes observed in human Huntington's disease brain and do not differ with mutant huntingtin length or wild-type huntingtin dosage. Hum. Mol. Genet. 16, 1845–1861.

Kroemer, G., Reed, J.C., 2000. Mitochondrial control of cell death. Nat. Med. 6, 513–519.

Liu, C.S., Cheng, W.L., Kuo, S.J., Li, J.Y., Soong, B.W., Wei, Y.H., 2008. Depletion of mitochondrial DNA in leukocytes of patients with poly-Q diseases. J. Neurol. Sci. 264, 18–21.

Mancuso, M., Orsucci, D., Siciliano, G., Murri, L., 2008. Mitochondria, mitochondrial DNA and Alzheimer's disease. What comes first? Curr. Alzheimer Res. 5, 457–468.

Milakovic, T., Johnson, G.V.W., 2005. Mitochondrial respiration and ATP production are significantly impaired in striatal cells expressing mutant huntingtin. J. Biol. Chem. 35, 30773–30782.

Morimoto, N., Nagano, I., Deguchi, K., Murakami, T., Fushimi, S., Shoji, M., Abe, K., 2004. Leber hereditary optic neuropathy with chorea and dementia resembling Huntington disease. Neurology 63, 2451–2552.

Oliveira, J.M., Chen, S., Almeida, S., Riley, R., Goncalves, J., Oliveira, C.R., Hayden, M.R., Nicholls, D.G., Ellerby, L.M., Rego, A.C., 2006. Mitochondrial-dependent Ca2+ handling in Huntington's disease striatal cells: effect of histone deacetylase inhibitors. J. Neurosci. 26, 11174–11186.

Onyango, I., Khan, S., Miller, B., Swerdlow, R., Trimmer, P., Bennett Jr., P., 2006. Mitochondrial genomic contribution to mitochondrial dysfunction in Alzheimer's disease. J. Alzheimers Dis. 9, 183–193.

Pang, Z., Geddes, J.W., 1997. Mechanisms of cell death induced by the mitochondrial toxin 3-nitropropionic acid: acute excitotoxic necrosis and delayed apoptosis. J. Neurosci. 17, 3064–3073.

Panov, A.V., Gutekunst, C.A., Leavitt, B.R., Hayden, M.R., Burke, J.R., Strittmatter, W.J., Greenamyre, J.T., 2002. Early mitochondrial calcium defects in Huntington's disease are a direct effect of polyglutamines. Nat. Neurosci. 5, 731–736.

Perluigi, M., Poon, H.F., Maragos, W., Pierce, W.M., Klein, J.B., Calabrese, V., Cini, C., De Marco, C., Butterfield, D.A., 2005. Proteomic analysis of protein expression and oxidative modification in r6/2 transgenic mice: a model of Huntington disease. Mol. Cell Proteomics 4, 1849–1861.

Rego, A.C., de Almeida, L.P., 2005. Molecular targets and therapeutic strategies in Huntington's disease. Curr. Drug Targets 4, 361–381.

Ruan, Q., Lesort, M., MacDonald, M.E., Johnson, G.V., 2004. Striatal cells from mutant huntingtin knock-in mice are selectively vulnerable to mitochondrial complex II inhibitor-induced cell death through a non-apoptotic pathway. Hum. Mol. Genet. 13, 669–681.

Sas, K., Robotka, H., Toldi, J., Vécsei, L., 2007. Mitochondria, metabolic disturbances, oxidative stress and kynurenine system, with focus on neurodegenerative disorders. J. Neurol. Sci. 257, 221–239.

Sawa, A., Wiegand, G.W., Cooper, J., Margolis, R.L., Sharp, A.H., Lawler, J.F.Jr, Greenamyre, J.T., Snyder, S.H., Ross, C.A., 1999. Increased apoptosis of Huntington disease lymphoblasts associated with repeat length-dependent mitochondrial depolarization. Nat Med. 10, 1194–1198.

Schapira, A.H., 1998. Mitochondrial dysfunction in neurodegenerative disorders. Biochim. Biophys. Acta 1366, 225–233.

Sorolla, M.A., Reverter-Branchat, G., Tamarit, J., Ferrer, I., Ros, J., Cabiscol, E., 2008. Proteomic and oxidative stress analysis in human brain samples of Huntington disease. Free Radic. Biol. Med. 45, 667–678.

Swerdlow, R.H., Parks, J.K., Cassarino, D.S., Shilling, A.T., Bennett Jr., J.P., Harrison, M.B., Parker Jr., W.D., 1999. Characterization of cybrid cell lines containing mtDNA from Huntington's disease patients. Biochem. Biophys. Res. Commun. 291, 701–704.

Tabrizi, S.J., Cleeter, M.W., Xuereb, J., Taanman, J.W., Cooper, J.M., Schapira, A.H., 1999. Biochemical abnormalities and excitotoxicity in Huntington's disease brain. Ann. Neurol. 45, 25–32.

Trottier, Y., Devys, D., Imbert, G., Saudou, F., An, I., Lutz, Y., Weber, C., Agid, Y., Hirsch, E. C., Mandel, J.L., 1995. Cellular localization of the Huntington's disease protein and discrimination of the normal and mutated form. Nat. Genet. 10, 104–110.

Turner, C., Cooper, J.M., Schapira, A.H., 2007. Clinical correlates of mitochondrial function in Huntington's disease muscle. Mov. Disord. 22, 1715–1721.

Vanlangenakker, N., Berghe, T.V., Krysko, D.V., Festjens, N., Vandenabeele, P., 2008. Molecular mechanisms and pathophysiology of necrotic cell death. Curr. Mol. Med. 8, 207–220.

Ward, M.W., Rego, A.C., Frenguelli, B.G., Nicholls, D.G., 2000. Mitochondrial membrane potential and glutamate excitotoxicity in cultured cerebellar granule cells. J. Neurosci. 20, 7208–7219.

Weber, A., Paschen, S.A., Heger, K., Wilfling, F., Frankenberg, T., Bauerschmitt, H., Seiffert, B.M., Kirschnek, S., Wagner, H., Häcker, G., 2007. BimS-induced apoptosis requires mitochondrial localization but not interaction with anti-apoptotic Bcl-2 proteins. J. Cell Biol. 177, 625–636.

Willis, S.N., Fletcher, J.I., Kaufmann, T., van Delft, M.F., Chen, L., Czabotar, P.E., Ierino, H., Lee, E.F., Fairlie, W.D., Bouillet, P., Strasser, A., Kluck, R.M., Adams, J.M., Huang, D.C., 2007. Apoptosis initiated when BH3 ligands engage multiple Bcl-2 homologs, not Bax or Bak. Science 315, 856–859.

Yang, J.-L., Weissman, L., Bohr, V., Mattson, M.P., 2008. Mitochondrial DNA damage and repair in neurodegenerative disorders. DNA Repair 7, 1110–1120.

Please cite this article as: Ferreira, I.L., et al., Mitochondrial-dependent apoptosis in Huntington's disease human cybrids, Exp. Neurol. (2010), doi:10.1016/j.expneurol.2010.01.002